Optimization of the Three-stage Biomass Gasification Characteristics in High-temperature Entrained-flow Bed

Chen Chao, Chunjiang Yu,* Jinsong Zhou, Yangyang Xiang, and Zhongyang Luo

The raw material requirements for the indirect liquefaction of biomass are strict. In particular, the ratio of H_2/CO must be greater than or equal to 1. However, traditional biomass gasification has problems that include a low H_2/CO ratio and low carbon conversion rates. This study proposes a three-stage gasification optimization model in which pyrolysis products are separated before being put through a second gasification step. The optimized model simulation used MATLAB software and the experiments were carried out in a biomass, high-temperature entrained-flow bed. The results demonstrate that, compared to traditional mixing gasification, three-stage gasification can effectively increase the H_2 content in syngas. The H_2 content can reach 42.3%, which is 4.6% higher than in traditional gasification. Additionally, this process can increase the H_2/CO ratio to 1.23, which is 43% higher than the ratio 0.86 in traditional gasification. This also could provide raw materials for the indirect liquefaction of syngas. Thus, three-stage gasification can eliminate the need for intermediate steps such as steam reforming and adding external H_2. Experiments indicated that the best gasification conditions were a first gasification time of 0.6s and a gasification temperature of 1100 °C, under which the H_2/CO ratio reached a maximum of 1.2.

Keywords: Biomass gasification; Staged gasification; Optimization model; High-temperature entrained-flow bed

*Contact information: State Key Laboratory of Clean Energy Utilization, Zhejiang University, Hangzhou 310027, China; *Corresponding author: chunjiang@cmee.zju.edu.cn*

INTRODUCTION

Biomass is the only renewable energy that can be converted into liquid fuels. In part because of its sustainability and carbon neutrality, the use of biomass as an alternative fuel source has received considerable attention around the world. Recently, biomass utilization technologies have developed rapidly. This is especially true of liquefaction technology used for the production of biomass-derived liquid fuels. These liquid fuels are a promising substitute for fossil fuels. Indirect biomass liquefaction is the process of synthesizing liquid fuels such as alcohols, ethers, and hydrocarbons from biomass-based syngas. The process involves the pretreatment of biomass, pyrolysis and gasification, gas purification, gas reforming, adjustment of the H_2/CO ratio, and methanol or dimethyl ether (DME) synthesis and separation, as shown in Fig. 1 (Songbai 2010). Biomass gasification for syngas production is a vital part of the overall system, for which the complexity and cost could be greatly reduced if the steam reforming and H_2/CO ratio adjustment steps could be omitted. This would be feasible if product gas from the gasifier met the requirements of a feed gas for Fischer-Tropsch synthesis.

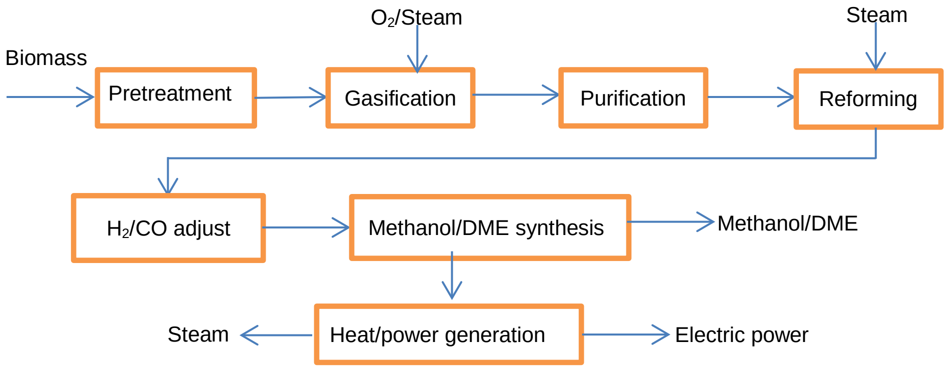

Fig. 1. Process schematic of methanol/DME synthesis

Biomass gasification is a thermochemical process that converts biomass into a gaseous product consisting mainly of H_2, CO, and CH_4. Gasification takes place at a specific temperature with oxygen or steam as the gasification agent. Ghaly *et al.* (Ghaly *et al.* 1988) first proposed the application of gasification technology to biomass fuels with a low energy density. After decades of development, researchers have developed a gasification gas supply system, gasification and synthetic liquid fuel system, gasification power generation system, and other such systems (Cocco *et al.* 2013; Trippe *et al.* 2011). Biomass gasification has turned toward fuels of higher calorific value and has become more selective and cleaner.

An oxygen-rich gasification system was examined (Wu *et al.* 1997), and the calorific value of the gaseous fuel produced by oxygen-rich gasification was found to be between 10 and 12 MJ/m^3, with a gasification efficiency above 70%. To reduce the cost, a 90% oxygen concentration was found to be sufficient. The oxygen consumption of the fuel was approximately 0.15 m^3/kg.

The syngas cleaning process is mainly employed for tar removal. Devi *et al.* (2003) studied and documented tar removal technology. The key points of primary treatment are (a) the proper selection of operating parameters, (b) the use of a bed additive/catalyst, and (c) gasifier modifications. The concepts of two-stage gasification and secondary air injection into the gasifier are of great importance to syngas cleaning. When the temperature reaches 1100 °C, the tar cracking reaction proceeds toward completion. If gasification medium is present and participates in the reaction, then the temperature for complete tar cracking is further reduced. In this study, it was reasonable to assume that the tar residue was negligible because of the small amount present during the high temperature gasification (Srinvas *et al.* 2013).

The pyrolysis and gasification reactions of alkali lignin can be catalyzed by NaOH and Na_2CO_3 (Guo *et al.* 2012). Chemicals such as alcohols, phenols, aldehydes, ketones, and hydrocarbons are responsible for the mass loss in the main pyrolysis stage and CO is the main gas released in the gasification stage.

A system of two-stage gasification (Henriksen *et al.* 2006), in which the primary reaction was divided into biomass pyrolysis and biomass gasification stages, was developed. The system power was 75 kW, and it could be continuously run for 465 h.

Xu *et al.* (2009) studied a two-stage dual fluidized bed gasification (T-DFBG) process that was thought to decrease tar production and increase gasification efficiency and H_2 production *via* an enhanced in-bed gas upgrading effect. Fuel pyrolysis and gasification occur in the lower stage of the two-stage fluidized bed (TFB) by interacting with the heat carrier particles (HCPs) from the upper stage and the gasification reagents (air and steam) fed into the stage (Xu *et al.* 2009).

The biomass gasification process consists of pyrolysis and gasification. The biomass is first decomposed into coke and volatile matter during the pyrolysis process. Then, O_2 reacts with H_2, CO, and CH_4 to generate H_2O and CO_2 during gasification. Finally, the O_2 residue reacts with the coke. The O_2 reacts with H_2 first because the reaction gases (O_2, H_2, CH_4, and others) are vigorously mixed and the activation energy of H_2 is lower than that of the coke. Therefore, the reaction of the gas mixture is faster than the reaction of O_2 with the coke. H_2 generated in the pyrolysis process first reacts with O_2 to generate H_2O, which then reacts with the coke to regenerate H_2, as shown in Fig. 2. This process causes energy losses during gasification. At the same time, it affects the gasification reaction by extending its duration.

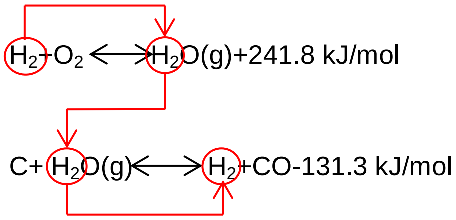

Fig. 2. Transfer of hydrogen in the biomass gasification reaction

To address the disadvantages of the above reactions, staged gasification was used to modify the traditional gasification reactions as shown in Fig. 3 (a). In this study, the products from the pyrolyzer were first separated into coke and volatiles. The coke was then reacted with the gasification agent in the first gasification stage, from which the pyrolysis gas (as shown in Table 1) was bubbled into the gasifier for the second gasification reaction, as shown in Fig. 3 (b). Simulations and experiments were used to optimize staged gasification for the production of syngas with an appropriate composition and H_2/CO ratio for Fischer-Tropsch synthesis.

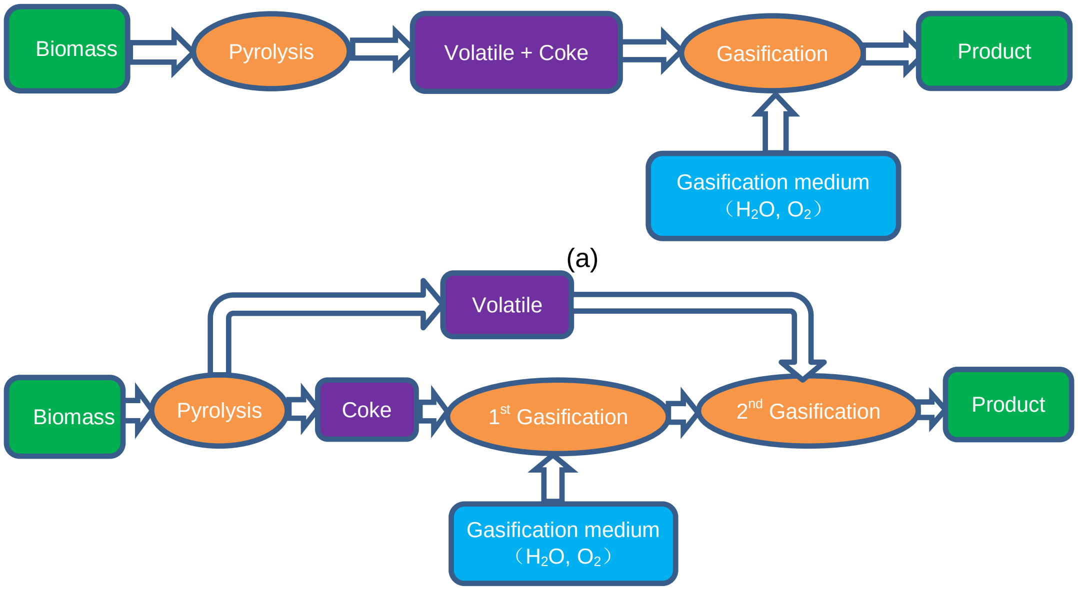

(a)

(b)

Fig. 3. Schematic diagram of biomass staged gasification

Table 1. Experimental Results of Sawdust Pyrolysis

Temperature (°C)	Component (vol. %)					
	H_2	CO	CO_2	CH_4	C_2H_4	C_2H_6
900	21.4835	40.6465	13.6575	13.8652	0.6548	0.6851
1000	25.9345	44.1588	12.8504	12.9672	0.4662	0.6247
1100	34.3721	44.7901	10.4799	7.7616	0.2373	0.3429
1200	37.9672	44.9766	8.9953	3.7383	0.0372	0.5128

EXPERIMENTAL

Equipment

Experiments were based on the biomass high-temperature entrained-flow bed gasification system illustrated in Fig. 4, which includes a biomass spiral feeding system, an oxygen preheating system, a steam generation system, the entrained-flow gasifier, an ash collection system, and the syngas purification and detection system. In the paper, the gasification experiment conditions were as specified in Table 3.

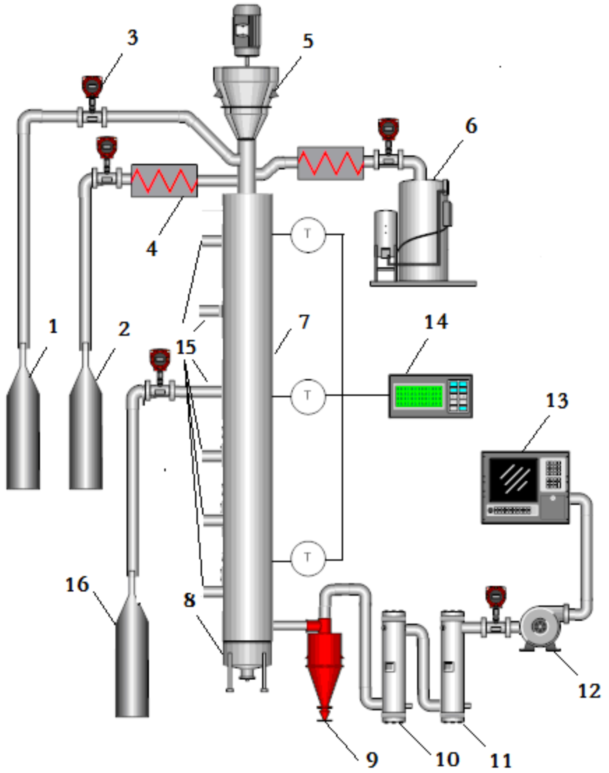

Fig. 4. Biomass high-temperature three-stage gasification system: 1-carrier gas; 2-gasification agent; 3-flowmeter; 4-preheater; 5-feeder; 6-steam generator; 7-gasifier; 8-ash hopper; 9-cyclone; 10-water scrubber; 11-drying oven; 12-air pump; 13-GC; 14-temperature controller; 15-sampling port and pyrolysis gas inlet; 16-simulated pyrolysis gas

Pyrolysis gas and charcoal were used to simulate biomass pyrolysis products. The influence of pyrolysis tar, which was present only at very low concentrations at high temperatures, was ignored. The charcoal industrial and elemental analyses are presented in Table 2, and the pyrolysis gas components are shown in Table 1. The pyrolysis gas used in the model was based on the components of a high-temperature pyrolysis gas. In this study, the feed amount of charcoal was confirmed as follows: the feed amount followed the law of mass conservation shown in Eq. (1) and the laws of elemental conservation shown in equations (2) and (3). The ash conservation principle (Pan and Eberhardt 2011) shown in Eq. (4) was also used. Equations (1), (2), (3), and (4) are as follows,

$$\dot{m}_{biomass} = \dot{m}_{charcoal} + \dot{m}_{pyrolysis-gas} \tag{1}$$

$$\dot{m}_{biomass} * W_C^{biomass} = \dot{m}_{charcoal} * W_C^{charcoal} + \dot{V}_{pyrolysis-gas} * \left(W_{CO} + W_{CO_2} + W_{CH_4}\right) \times \frac{12}{22.4} \tag{2}$$

$$\dot{m}_{biomass} * \dot{W}_H^{biomass} = m_{charcoal} * W_H^{charcoal} + \dot{V}_{pyrolysis-gas} * \left(W_{H_2} + 2 * W_{CH_4}\right) \times \frac{2}{22.4} \tag{3}$$

$$\dot{m}_{biomass} * W_A^{biomass} = \dot{m}_{charcoal} * W_A^{charcoal} \tag{4}$$

Table 2. Ultimate and Proximate Analysis of Feed Stock

Material	Ultimate analysis (air-dried, wt. %)					Proximate analysis (air-dried, wt. %)			
	C	H	O	N	S	M	A	V	FC
Sawdust	48.88	6.29	31.27	1.7	0.06	7.86	3.94	70.14	18.06
Charcoal	45.27	2.32	11.19	1.07	0.04	6.84	32.22	19.68	40.2
coke	46.33	1.52	6.34	0.77	0.09	7.26	37.69	11.5	43.55

Table 3. Experimental Gasification Conditions

Gasification condition	Result
Flux of feeding	150 g/h
Carrier gas	200 L/h
Ratio of oxygen to biomass (O_2/B)	0.5
Ratio of steam to biomass (S/B)	0.3
Total gasification time	2 s
Time of first gasification	0 to 1.4s
Temperature of the whole gasification process	800 to 1400 °C

Three-level Quasi-equilibrium Gasification (TQEG) Model

A three-level quasi-equilibrium gasification model was recently proposed by Nguyen *et al.* (2012). The three stages are a biomass pyrolysis stage, a carbon-gas reaction stage, and a water-gas reaction stage. They were proposed to simulate the entire biomass gasification process in a fluidized bed. All the phases of each stage must be calculated before the result is input into the next stage. The characteristic parameters for each stage in the process were simulated and proposed in Fig. 5.

According to the three-level quasi-equilibrium gasification model, this study focused on the optimization of the traditional gasification model, which is divided into three parts: biomass pyrolysis, gasification of coke, and the gas reforming reaction, as shown in Fig. 3 (b). The first phase is the pyrolysis of the biomass, which mainly consists of the volatile matter and the cracking of tar (macromolecular aromatic hydrocarbons).

The second stage is the gasification reaction between the biomass char and the gasification medium, oxygen or water vapor. At this stage, coke consumption is rapid. The last stage is based on the amounts of residual coke and gas, which are bubbled into the pyrolysis gas and the gasification medium (H_2O) for a second consumption of coke. During this stage, the syngas composition is adjusted to improve the carbon conversion rate, adjust the H_2/CO ratio, and to reduce energy consumption.

Table 4. Reactions and Products of the Three-level Quasi-equilibrium Gasification Model

Stage	Reaction(s)	Products
Pyrolysis	First step: thermal decomposition Second step: tar cracking	CO, CO_2, CH_4, H_2, C_2H_4,C_2H_6, H_2O
Solid-water reactions	$C(s)+O_2(g) \leftrightarrow CO_2(g)$ $C(s)+CO_2(g) \leftrightarrow CO(g)$ $C(s)+H_2O(g) \leftrightarrow CO(g)+H_2(g)$ $C(s)+2H_2O(g) \leftrightarrow CO_2(g)+2H_2(g)$	Char (un-reacted), CO, CO_2, H_2, CH_4, H_2O residue
Water-gas shift reaction	$CO(g)+H_2O(g) \leftrightarrow CO_2(g)+H_2(g)$ $CO_2(g)+CH_4(g) \leftrightarrow CO(g)+H_2(g)$ $C(s)+CO_2(g) \leftrightarrow CO(g)$ $C(s)+2H_2O(g) \leftrightarrow CO_2(g)+2H_2(g)$	CO, CO_2, H_2, CH_4, H_2O

The TQEG model was validated with experimental data obtained from high-temperature biomass gasification in an entrained-flow bed. A parametric study of T_G and t_1 was performed to predict the final gas composition W_i, the carbon conversion $Ø_C$, the gasification efficiency η (Zhao, 2007), the H_2/CO molar ratio $Ø_{H2/CO}$, and the CO/CO_2 molar ratio $Ø_{CO/CO2}$. Figure 5 summarizes the structure of the TQEG model and the scope of the parametric study.

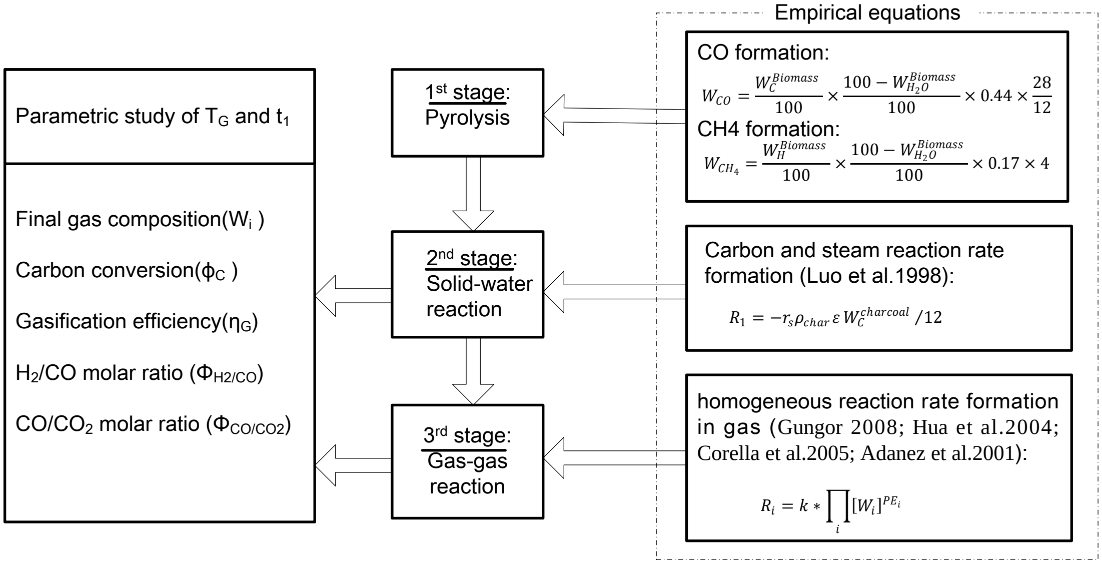

Fig. 5. Parametric study and empirical equations

RESULTS AND DISCUSSION

This study explored the gasification characteristics of staged gasification *via* both simulation and experimentation. First, a comparative study of different gasification methods, including traditional sawdust gasification, charcoal gasification, an optimized gasification model, and first gasification mixed with volatiles (charcoal gasification with a mixed pyrolysis gas) was carried out. The effects of various parameters on gasification at temperatures from 800 to 1400 °C were then investigated. Finally, the influence of the residence time within the first gasification stage on the overall performance of the whole system was studied.

Comparison of the Gasification Models

First, the gasification temperature was set at 1000 °C. The syngas composition with different gasification models was determined in this study, as shown in Fig. 6. It is clear that the hydrogen content and the carbon conversion rate of charcoal gasification were higher than those of the other three methods. This is due to a higher fixed carbon content (shown in Table 2), which could enhance the reaction between the carbon and steam. Furthermore, the H_2/CO ratio in charcoal gasification was highest (approximately 1.4), as shown in Fig. 7, which is advantageous to the whole gasification system. The charcoal gasification method is the best method for achieving directional gasification, at least superficially. However, charcoal production requires large amounts of energy, and a large amount of the pyrolysis gas produced in this process is wasted. Therefore, an optimal model that takes advantage of coal gasification and reuses the pyrolysis gas is of great value. Such a model was the main focus of this study.

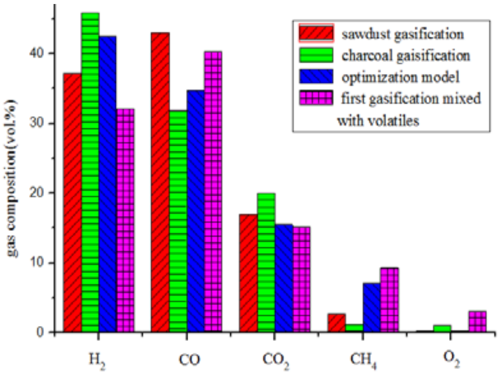

Fig. 6. Composition of different gasification models

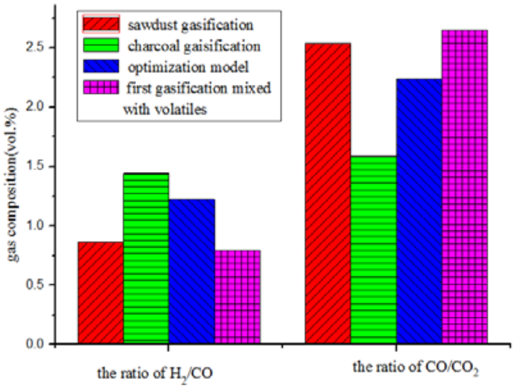

Fig. 7. H_2/CO and CO/CO_2 ratios in different gasification models

As shown in Figs. 6 and 7, the hydrogen content in the optimized model was slightly lower than in charcoal gasification but was still higher than in the other gasification methods. The H_2/CO ratio was also as high as 1.2, reaching the goal of directional gasification. Finally, this study examined the mixture components of the charcoal gasification syngas mixed with pyrolysis gas. Results indicated that this method utilized the pyrolysis gas but was unsatisfactory because the hydrogen content was even lower than that obtained with ordinary gasification.

Influence of Gasification Temperature

Because temperature is an important gasification parameter, the influences of an increase in temperature from 800 to 1400 °C on the changes in the H_2/CO ratio and syngas composition were investigated in this study.

Figure 8 illustrates the change in the composition of syngas with temperature. Both the simulations and the experiments indicate that the H_2 content increases with rising temperature and the CO content falls after rising initially. The maximum value for the CO content appeared between 1100 and 1200 °C because CO is formed by the reaction between hot coke and water vapor, which more readily occurs at temperatures above 1100 °C. However, the change in CO_2 was contrary to that of the CO content, which could be because the rate of reaction (1) was greater at higher temperatures and generated large amounts of CO_2 and H_2. At the same time, a high temperature and high levels of water vapor promote the water-gas reaction (2), and as a result, the CO_2 content increases and the CO content decreases.

$$C(s)+2H_2O(g) \longleftrightarrow CO_2(g)+2H_2(g)-90.1\ \text{kJ/mol} \quad (1)$$

$$CO(g)+H_2O(g) \longleftrightarrow CO_2(g)+H_2(g)+41.2\ \text{kJ/mol} \quad (2)$$

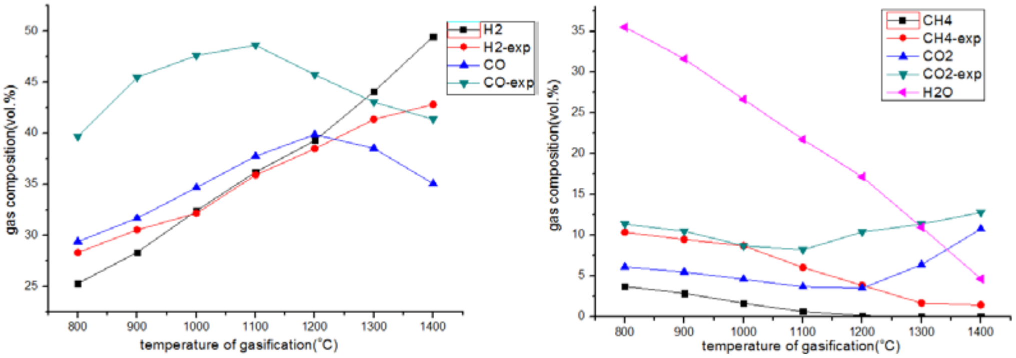

（a） （b）

Fig. 8. Change in the composition of syngas with temperature

The influence of gasification on the H_2/CO ratio is illustrated in Fig. 9. The H_2/CO ratio rises with increasing temperature. A sharper trend can be observed at temperatures over 1200 °C, which is the result of further completion of reaction (1). Although directional gasification is aimed at obtaining a larger H_2/CO ratio, energy consumption and CO_2 emissions should be also taken into consideration.

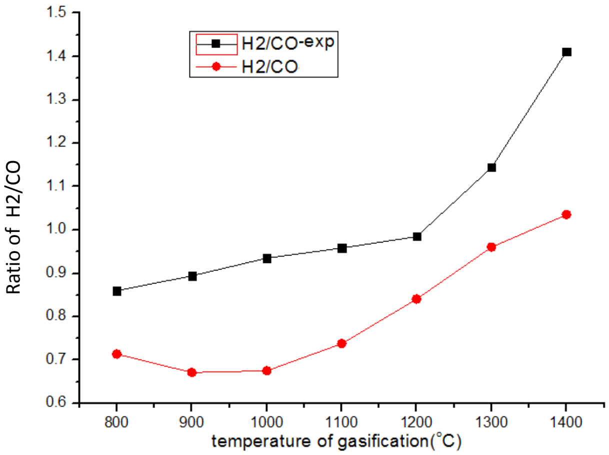

Fig. 9. Change in the H_2/CO ratio with temperature

Effect of First Gasification Time on the Gasification Result

While maintaining a constant total residence time, the effect of changes in residence time in the first gasification stage on the performance of gasification was investigated. Variations in the gasification syngas and the H_2/CO ratio with increasing first gasification residence time are shown in Fig. 10, in which figures (a) and (b) are the simulation results and figures (c) and (d) are the experimental results.

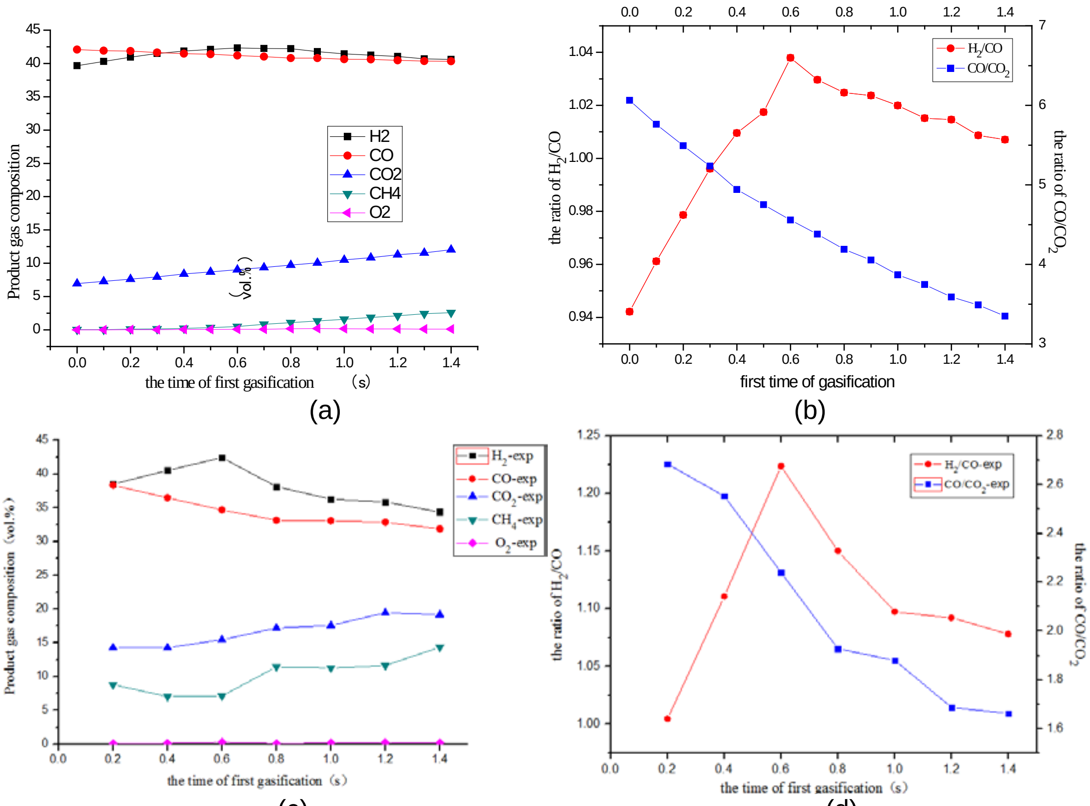

(a) (b)

(c) (d)

Fig. 10. Influence of first gasification time on syngas composition

As shown in Fig. 10, the CO content decreased and H_2 exhibited a decreasing trend after the first rise. The other components exhibited an increasing trend. With a gasification time of 0.6 s, the H_2/CO ratio reached a maximum of 1.2 and then decreased rapidly with increasing gasification time, as shown in Figs. 10 (b) and (d). This is due to the greater reducibility of H_2. The consumption rate of H_2 *via* reaction (3) gradually surpassed the H_2 generation rate with increasing first gasification time because the H_2 concentration increased first and then decreased with increasing first gasification time.

$$H_2\,(g)+O_2\,(g) \longleftrightarrow H_2O(g)+241.8\ \text{kJ/mol} \qquad (3)$$

The time of first gasification also affects the carbon conversion rate and gasification efficiency, as shown in Fig. 11. The carbon conversion rate reached 96.3% at the time of 1.2s. That was because of the reaction of carbon and oxygen. But when the first gasification time more than 1.2 s, the reaction of hydrogen and oxygen hold dominant position. The gasification efficiency attained 74.5% at the time of 1.0 s.

From the data it can be seen that the simulation and experimental results had a consistent trend, but the lines had a little distance. There were two reasons for this. First, the charcoal and the coke had the different amounts of components, especially the fixed carbon and volatile matter. The second reason was the partial mixing between the first gasification and second gasification. This still needs further research related to the modification of the gasifier.

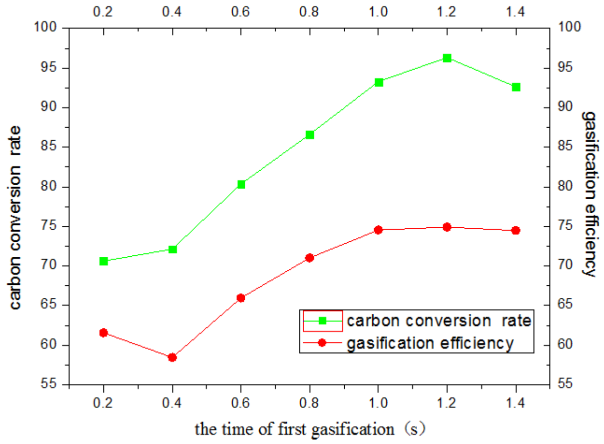

Fig. 11. Carbon conversion rate and gasification efficiency as functions of first gasification time

CONCLUSIONS

1. Compared to traditional mixing gasification, three-stage gasification can enhance the H_2 content in syngas. The H_2 content reached 42.3%, which is 4.6% higher than in traditional gasification.
2. This method can increase the H_2/CO ratio to 1.23, which is 43% higher than in traditional gasification, which means it could provide feed for liquid fuel production.
3. The three-stage gasification optimization model innovatively suggests that the pyrolysis gas be passed into the second stage of the three-stage gasification model. The simulation results and the experimental results are consistent trend. This method could eliminate the need for the intermediate steps of steam reforming and adding extra hydrogen.

4. Both the simulation and the experiments indicate that the best gasification condition for three-stage gasification is a first gasification time of 0.6 s with a gasification temperature of 1100 °C. Under these conditions, the H_2/CO ratio could reach a maximum of 1.2.

ACKNOWLEDGMENTS

The authors are grateful for the support of the National Basic Research Program of China (no. 2013CB228100), and the State Key Program of National Natural Science of China (no. 51336008).

NOMENCLATURE

A	Ash content in material obtained by proximate analysis (wt. %)
FC	Fixed carbon content in material obtained by proximate analysis (wt. %)
M	Moisture content in material obtained by proximate analysis (wt. %)
$\dot{m}_{biomass}$	Biomass feed rate (kg/h)
$\dot{m}_{charcoal}$	Charcoal feed rate (kg/h)
$\dot{m}_{pyrolysis-gas}$	Pyrolysis gas feed rate (kg/h)
$W_C^{biomass}$	Carbon content in biomass (wt. %)
$W_C^{charcoal}$	Carbon content in charcoal (wt. %)
W_{CO}	Carbon monoxide volume content in pyrolysis gas (vol. %)
W_{CO_2}	Carbon dioxide volume content in pyrolysis gas (vol. %)
W_{CH_4}	Methane volume content in pyrolysis gas (vol. %)
$W_H^{biomass}$	Hydrogen content in biomass (wt. %)
$W_H^{charcoal}$	Hydrogen content in charcoal (wt. %)
W_{H_2}	Hydrogen content in pyrolysis gas (vol. %)
$W_{H_2O}^{biomass}$	Water content in biomass or water value in biomass proximate analysis (kg/kg)
$W_A^{biomass}$	Ash content in biomass (wt. %)
$W_A^{charcoal}$	Ash content in charcoal (wt. %)
W_i	Content of all components in gasification gas (vol. %)
V	Volatile content in material obtained by proximate analysis (wt. %)
$\dot{V}_{pyrolysis-gas}$	Pyrolysis gas feed volumetric flow rate (Nm^3/h)
T_G	Temperature of the entire gasification process (°C)
R_1	Reaction rate of the carbon and steam reaction (mol/s)
R_i	Reaction rate of every reaction between gases (mol/s)
PE_i	Power exponent of every reaction between gases
$\emptyset_C$	Carbon conversion (wt. %)
η_G	Gasification efficiency of whole process (kJ/kJ)
$\emptyset_{H2/CO}$	H_2/CO molar ratio in gasification gas (mol/mol)
$\emptyset_{CO/CO2}$	CO/CO_2 molar ratio in gasification gas (mol/mol)

t_1	The time of biomass gasification in solid-water reaction stage (s)
r_s	Carbon and steam reaction rate controlled by chemistry (mol/s)
ρ_{char}	Grain density in reaction (kg/m^3)
ε	Average void space in entrained flow bed (0.95 in this model)
κ	The constant regarding property and temperature of reactant is usually expressed as the Arrhenius law

REFERENCES CITED

Adanez, J., Gayán, P., Grasa, G., de Diego, L. F., Armesto, L., and Cabanillas, A. (2001). “Circulating fluidized bed combustion in the turbulent regime: Modelling of carbon combustion efficiency and sulphur retention,” *Fuel* 80(10), 1405-1414.

Cocco, D., Serra, F., and Tola, V. (2013). “Assessment of energy and economic benefits arising from syngas storage in IGCC power plants,” *Energy* 58, 635-643.

Corella, J., and Sanz, A. (2005). “Modeling circulating fluidized bed biomass gasifiers. A pseudo-rigorous model for stationary state,” *Fuel Proc. Technol.* 86(9), 1021-1053.

Devi, L., Ptasinski, K. J., and Janssen, F. J. J. G. (2003). “A review of the primary measures for tar elimination in biomass gasification processes,” *Biomass and Bioenergy* 24(2), 125-140.

Gahly, M., Piskorz, J., Scott, D. S., and Radlein, D. (1988). “The hydro gasification of wood,” *Industrial Engineering Chemistry Research* 27(2), 256-264.

Gungor, A. (2008) “Two-dimensional biomass combustion modeling of CFB,” *Fuel* 87(8-9), 1453-1468.

Guo, D.-L., Wu, S.-B., Liu, B., Yin, X.-L., and Yang, Q. (2012). “Catalytic effects of NaOH and Na_2CO_3 additives on alkali lignin pyrolysis and gasification,” *Applied Energy* 95, 22-30.

Henriksen, U., Ahrenfeldt, J., Jensen, T. K., Gobel, B., Bentzen, J. D., Hindsgaul, C., and Sorensen, L. H. (2006). “The design, construction and operation of a 75 kW two-stage gasifier,” *Energy* 31(10-11), 1542-1553.

Hua, Y., Flamant, G., Lu, J., and Gauthier, D. (2004). “Modelling of axial and radial solid segregation in a CFB boiler,” *Chem. Eng. Processing* 43(8), 971-978.

Luo, C.-H., Aoki, K., Uemiya, S., and Kojima, T. (1998). “Numerical modeling of a jetting fluidized bed gasifier and the comparison with the experimental data,” *Fuel Processing Technology* 55(3), 193-218.

Nguyen, T. D. B., Ngo, S. I., Lim, Y.-I., Lee, J. W., Lee, U.-D., and Song, B.-H. (2012). “Three-stage steady-state model for biomass gasification in a dual circulating fluidized-bed,” *Energy Conversion and Management* 54(1), 100-112.

Pan, H., and Eberhardt, T. L. (2011). “Characterization of fly ash from the gasification of wood and assessment for its application as a soil amendment,” *BioResources* 6(4), 3987-4004.

Songbai, Q. (2010). *Study on Production of Clean Biofuel using Bio-syngas.* University of Science and Technology of China, Hefei City, China.

Srinvas, S., Field, R. P., and Herzog, H. J. (2013). “Modeling tar handling options in biomass gasification,” *Energy Fuel* 27(6), 2859-2873.

Trippe, F., Fröhling, M., Schltmann, F., Stahl, R., and Henrich, E. (2011). “Techno-economic assessment of gasification as a process step within biomass-to-liquid (BtL) fuel and chemicals production,” *Fuel Processing Technology* 92(11), 2169-2184.

Wu, C., Xu, B., Luo, Z., Yin, X., and Liu, P. (1997). "Design and operation of biomass gasification device for middle heat value gas,"*Acta Energiae Solaris Sinica* 1(18), 1-6.
Xu, G., Murakami, T., Suda, T., Matsuzaw, Y., and Tani, H. (2009). "Two-stage dual fluidized bed gasification: Its conception and application to biomass," *Fuel Processing Technology* 90(1), 137-144.
Zhao, H. (2007). *Experimental and Mechanism Research on Entrained Flow Gasification of Biomass for Syn-gas*. Zhejiang University, Hangzhou city, China.

Article submitted: January 6, 2014; Peer review completed: February 21, 2014; Revised version received: February 25, 2014; Accepted: March 5, 2014; Published: March 24, 2014.